

## Photoionization of excited states of neon-like Mg III

NARENDRA SINGH and MAN MOHAN

Department of Physics and Astrophysics, Delhi University, Delhi 110 007, India

Email: nsingh76@yahoo.co.in; sneh@del2.vsnl.net.in

MS received 26 February 2001; revised 10 September 2001

**Abstract.** The close coupling  $R$ -matrix method is used to calculate cross-sections for photoionization of Mg III from its first three excited states. Configuration interaction wave functions are used to represent two target states of Mg III retained in the  $R$ -matrix expansion. The positions and effective quantum numbers for the Rydberg series converging to the excited state  $2s^2 2p^6 \ ^2S^e$  of the residual ion, are predicted.

**Keywords.** Photoionization; configuration interaction;  $R$ -matrix method.

**PACS Nos** 32.80.-t; 32.80.fb

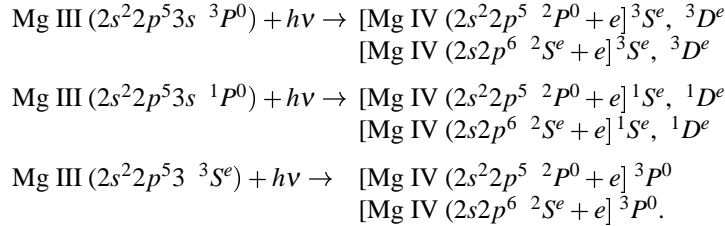
### 1. Introduction

Recently there is a great interest in accurate calculation of photoionization cross-section of positive ions due to their importance in interpreting the spectral lines arising in fusion [1] and astrophysical plasma [2,3]. Also in the X-ray laser research, photoionization of neon-like ions has found application in understanding the resonant photopumping scheme for driving lasing action [3]. Recently, neon-like aluminium ions produced by Z-pinch plasma were used in vacuum ultra-violet lasing [4] and also soft X-ray laser simulation for neon-like krypton ions by an electron pumping scheme in Z-pinch plasma condition was reported [5,6]. The magnesium absorption spectra, when recorded in the early stages of plasma history, exhibit numerous lines of Mg III ion and a Rydberg series arising from excitation of an inner electron has been observed in neon-like magnesium by Esteva and Mehlman [7]. Mohan *et al* [8,9] and recently Chakraborty *et al* [10] have also done work on photoionization of some neon-like ions including Mg III but only near threshold.

In the present work we have used the close coupling  $R$ -matrix method [8,11] to obtain accurate photoionization cross-section from the first three excited  $1s^2 2s^2 2p^5 3s \ ^3P^0$ ,  $1s^2 2s^2 2p^5 3p \ ^3S^e$  states of Mg III, allowing for the residual ion to be left in one of the two lowest states Mg IV:  $1s^2 2s^2 2p^5 \ ^2P^0$ ,  $1s^2 2s^1 2p^6 \ ^2S^e$ . These target states are represented by configuration interaction (CI) wave functions described in detail by Mohan and Hibbert [9].

## 2. Calculations

In the present paper we have calculated the photoionization cross-section from the first three excited  $1s^2 2s^2 2p^5 3s^3 \ ^1P^0$ ,  $1s^2 2s^2 2p^5 3p^3 \ ^3S^e$  states of Mg III for photon energies ranging from the ground state ionization threshold to the first excited threshold. At these energies, only the channel associated to the first two states  $1s^2 2s^2 2p^5 \ ^2P^0$  and  $1s^2 2s^2 2p^6 \ ^2S^e$  of Mg IV are open. These photoionization processes from the first three excited states of Mg III up to  $^2S^e$  threshold of Mg IV can therefore be described as



In the  $R$ -matrix formulation of photoionization, the initial bound state  $i$  of Mg III and the final continuum state  $f$  of the residual ion Mg IV plus outgoing electron are expanded consistently on collision type  $R$ -matrix basis sets, expressed in terms of the state of the  $N$ -electron residual ion Mg IV.

The two lowest  $LS$  states of the Mg IV target are represented by configuration expansion [12] as

$$\Phi(LS) = \sum_{i=1}^M a_i \phi_i(\alpha_i, LS), \quad (1)$$

where the single configuration function  $\phi_i$  are constructed from one electron orbitals, whose angular momenta are coupled as specified by  $\alpha_i$  to form states of given total  $L$  and  $S$ . The radial part of each orbital is written as a linear combination of normalized Slater-type orbitals (STO).

$$P_{nl}(r) = \sum_{i=1}^k c_i r^{p_i} \exp(-\zeta_i r). \quad (2)$$

The parameter  $\{c_i\}$ ,  $\{p_i\}$  and  $\{\zeta_i\}$  in eq. (2) are determined variationally as described by Hibbert *et al* [13].

In the present calculation, we have restricted basis of 3 STOS  $1s$ ,  $2s$  and  $2p$  optimized on the ground state by Clementi and Roetti [14] while  $3s$ ,  $3p$  and  $3d$  were obtained by us as described by Hibbert *et al* [13]. We have represented the two Mg IV  $LS$  states included in the calculation as described by eq. (1). In table 1, we have listed the configurations used in the CI expansion of the Mg IV states, while in table 2, we have compared our theoretical energy separations between the Mg IV states included in the collisional calculation, with the experimental ones, compiled by Martin and Zalubus [15].

The initial and final continuum wave functions used for the photoionization of  $(N + 1)$  electron system are expanded in the inner configuration space  $r \leq a$ , as described by Burke *et al* [11], in terms of discrete  $R$ -matrix basis functions of adequate  $LS$  symmetry.

**Table 1.** Configuration used in the CI expansion of Mg IV.

Target states	Key no.	Configuration used
$2P^0$	1	$[1s^2] 2s^2 2p^5, 2s^2 2p^4(^3P^e)3p, 2s^2 2p^4(^1D^e)3p, 2s^2 2p^4(^1S^e)3p, 2p^5(^1P^0)3s^2, 2p^5(^3P^0)3s^2$
$2S^e$	2	$[1s^2] 2s 2p^6, 2s 2p^5(^1P^0)3s, 2s 2p^5(^3P^0)3s, 2s 2p^5(^1P^0)3d, 2s 2p^5(^1P^0)3p, 2s 2p^5(^3P^0)3p$

**Table 2.** Excitation threshold for Mg IV.

Key no.	Configuration	State	Energy in Rydberg	
			Theory	Expt.
1	$1s^2 2s^2 2p^5$	$2P^0$	0.00000	0.00000
2	$1s^2 2s 2p^6$	$2S^e$	2.96292	2.83845

$$\psi_k^{LS\pi} = A \sum_{ij} C_{ijk} \Phi_i^{LS\pi}(X_1 \dots X_N \cdot \mathbf{r}_{N+1}, \sigma_{N+1}) u_{ij}(\mathbf{r}_{N+1}) + \sum_j d_{jk} \phi_j(X_1 \dots X_{N+1}) \quad (3)$$

inside a sphere of radius  $a$ , containing the charge distribution of the residual ion in (3),  $A$  is the antisymmetrization operator which account for electron exchange,  $\Phi_i$  are channel functions formed by coupling the target state of coordinates  $x_i = \{r_i, \mathbf{r}_i, \sigma_i\}$  with the spin angle function of the scattered electron in order to form eigenstates of  $L, S$  and parity  $\pi_i$ .

The  $(u_{ij})$  form a discrete  $R$ -matrix basis of continuum orbitals for scattered electron and the  $\{\Phi_j\}$  are  $\{N + 1\}$  electron bound configurations, which account for the orthogonality of the continuum orbitals  $u_{ij}$  to the bound orbitals. The continuum orbitals  $u_{ij}$  in (3) are eigenfunctions of a zero-order non-relativistic model Hamiltonian.

$$\left[ \frac{d^2}{dr^2} + \frac{l_i(l_i + 1)}{r^2} + 2V(r) - k_i^2 \right] u_{ij}(r) = \sum_k \lambda_{ijk} P_k(r) \quad (4)$$

which satisfy the boundary conditions

$$u_{ij} = 0, \quad (5a)$$

$$\frac{a}{u_{ij}} \frac{du_{ij}}{dr} \Big|_{r=a} = b. \quad (5b)$$

In eq. (4)  $l_i$  is the angular momentum of the scattered electron,  $V(r)$  is the static potential of the target in its ground state, and  $\lambda_{ijk}$  are Lagrange multipliers, which are determined in order to ensure the orthogonality of the continuum orbitals to the bound radial orbitals  $P_{kl}(r)$  having the same angular momentum  $l_i$ .  $R$ -matrix theory starts by partitioning configuration space into two regions by a sphere of radius  $a$  centered on the target nucleus [16]. In the external region  $r > a$ , electron exchange between the scattered electron and

target can be neglected if the radius  $a$  is chosen large enough so that the charge distribution of the target is contained within the sphere [17]. Therefore, the  $N$ -electron target orbitals must become vanishingly small in the external region. The boundary radius  $a$  is chosen in the external region. The boundary radius  $a$  is chosen such that [18]  $|P_{nl}(r=a)| < \delta$  for all bound orbitals included in the calculation, where  $\delta$  is a small number, e.g.  $\delta$  is of the order of  $10^{-4}$  a.u. We have imposed a zero logarithmic derivative  $b = 0$  at the  $R$ -matrix boundary radius  $a = 4.0$  a.u. and retained 10 continuum orbitals for each angular symmetry to ensure convergence in the energy range considered here.

The coefficients  $C_{ijk}$  and  $d_{jk}$  in (3) were determined by diagonalizing the  $(N + 1)$  electron Hamiltonian in the inner region. In the outer region ( $r \geq a$ ), the radial equations were solved, assuming a purely Coloumbic asymptotic interaction.

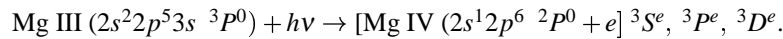
Finally, the differential cross-section for photoionization of an  $(N + 1)$  electron atom with the electron ejected in direction  $\vec{k}$  and the ion left in the state  $f$  is given by

$$\frac{d\sigma_f}{d\vec{k}} = 8\pi^2 \alpha a_0^2 \omega \left| \left\langle \psi_i(\vec{k}) \left| \sum_{i=1}^{N+1} \vec{r}_i \right| \psi_i \right\rangle \right|^2, \quad (6)$$

where  $\omega$  is the photon energy in a.u.,  $\alpha$  is the fine structure constant,  $a_0$  is the Bohr radius,  $\psi_i$  is the wave function of the initial bound state and  $\psi_f(\vec{k})$  is the wave function of the final state with the single outgoing wave corresponding to the ejected electron in the direction  $\vec{k}$  and the residual ion in state  $f$ .

### 3. Results and discussion

The cross-section for photoionization of the first three excited  $1s^2 2s^2 2p^5 3s^3 \ ^{3,1}P^0$ ,  $1s^2 2s^2 2p^5 3p^3 \ ^{3}S^e$  are obtained in  $LS$  coupling. Only the length results are given throughout the paper. If exact wave functions are used the length and velocity cross-sections are identical. However, in general, length and velocity formulas give different results and the magnitude of the difference is often used as an indication of the accuracy of the approximations. As discussed by Starace [19,20] length results are preferred to velocity results. Our results are near to each other within 10%. In figures 1 and 2 we have displayed the total photoionization cross-section for photoionization from the first excited  $1s^2 2s^2 2p^5 3s^3 \ ^{3}P^0$  state of Mg III. The  $^3S^e$ ,  $^3D^e$  and  $^3P^e$  final states are allowed by dipole selection rule for photoionization from this state. This process can be represented as



It is to be noted that the final  $^3P^e$  state does not couple to the  $^3P^0$  excited state and therefore do not have any closed channel resonances below this threshold. Here as expected we find two Rydberg series  $[\text{Mg IV } (2s^1 2p^6 \ ^{2}S^e)ns] \ ^{3}S^e$  and  $[\text{Mg IV } (2s^1 2p^6 \ ^{2}S^e)nd] \ ^{3}D^e$  converging to  $^2S^e$  threshold as allowed by angular momentum and parity conservation rules. The position and effective quantum numbers for these resonances are given in table 3. Here in figure 1 we find one interesting phenomena that the first peak corresponding to autoionized resonance  $(2s^1 2p^6) \ ^{2}S^e \ 3s^3 \ ^{3}S^e$  is very large as compared to other peaks



**Table 3.** Resonance position and effective quantum numbers for the Rydberg series Mg III ( $[1s^2]2s2p^6\ ^2S^e\ ns\ ^3S^e$ ) and ( $[1s^2]2s2p^6\ ^2S^e\ nd\ ^3D^e$ ) converging to  $2s2p^6\ ^2S^e$  limit of Mg IV.

Ionization potential of Mg III ( $[1s^2]2s2p^63s\ ^3P^0$ ) Ryd.			Threshold of Mg IV ( $[1s^2]2s2p^6\ ^2S^e$ ) Ryd.	
Theory 1.9898			Theory 4.9527	
Series	Limit	Configuration	Resonance position	Effective quantum number ( $n^*$ )
$^3S^e$	$[1s^2]2s2p^6\ ^2S^e$	$[1s^2]2s2p^63s$	3.0104	2.15
		$[1s^2]2s2p^64s$	4.0490	3.16
		$[1s^2]2s2p^65s$	4.4324	4.16
		$[1s^2]2s2p^66s$	4.6142	5.16
		$[1s^2]2s2p^67s$	4.7150	6.15
		$[1s^2]2s2p^68s$	4.7762	7.14
$^3D^e$	$[1s^2]2s2p^6\ ^2S^e$	$[1s^2]2s2p^63d$	3.9445	2.95
		$[1s^2]2s2p^64d$	4.3874	3.99
		$[1s^2]2s2p^65d$	4.5872	4.96
		$[1s^2]2s2p^66d$	4.6988	5.95
		$[1s^2]2s2p^67d$	4.7672	6.96
		$[1s^2]2s2p^68d$	4.8104	7.95

**Table 4.** Resonance position and effective quantum numbers for the Rydberg series Mg III ( $[1s^2]2s2p^6\ ^2S^e\ ns\ ^1S^e$ ) and ( $[1s^2]2s2p^6\ ^2S^e\ nd\ ^1D^e$ ) converging to  $2s2p^6\ ^2S^e$  limit of Mg IV.

Ionization potential of Mg III ( $[1s^2]2s2p^63s\ ^1P^0$ ) Ryd.			Threshold of Mg IV ( $[1s^2]2s2p^6\ ^2S^e$ ) Ryd.	
Theory 1.9438			Theory 4.9067	
Series	Limit	Configuration	Resonance position	Effective quantum number ( $n^*$ )
$^1S^e$	$[1s^2]2s2p^6\ ^2S^e$	$[1s^2]2s2p^63s$	3.0328	2.19
		$[1s^2]2s2p^64s$	4.0246	3.19
		$[1s^2]2s2p^65s$	4.3972	4.20
		$[1s^2]2s2p^66s$	4.5754	5.21
		$[1s^2]2s2p^67s$	4.6762	6.24
		$[1s^2]2s2p^68s$	4.7338	7.21
$^1D^e$	$[1s^2]2s2p^6\ ^2S^e$	$[1s^2]2s2p^63d$	3.9122	2.97
		$[1s^2]2s2p^64d$	4.3432	3.99
		$[1s^2]2s2p^65d$	4.5430	4.97
		$[1s^2]2s2p^66d$	4.6528	5.95
		$[1s^2]2s2p^67d$	4.7212	6.96
		$[1s^2]2s2p^68d$	4.7644	7.95

**Table 5.** Resonance position and effective quantum numbers for the Rydberg series Mg III ( $[1s^2]2s2p^6\ ^2S^e\ np\ ^3P^0$ ) and converging to  $2s2p^6\ ^2S^e$  limit of Mg IV.

Ionization potential of Mg III ( $[1s^2]2s2p^63p\ ^3S^e$ ) Ryd.		Threshold of Mg IV ( $[1s^2]2s2p^6\ ^2S^e$ ) Ryd.		
Theory 1.6270		Theory 4.5899		
Series	Limit	Configuration	Resonance position	Effective quantum number ( $n^*$ )
$^3P^0$	$[1s^2]2s2p^6\ ^2S^e$	$[1s^2]2s2p^63p$	3.0742	2.44
		$[1s^2]2s2p^64p$	3.8284	3.44
		$[1s^2]2s2p^65p$	4.1362	4.45
		$[1s^2]2s2p^66p$	4.2874	5.45
		$[1s^2]2s2p^67p$	4.3756	6.48
		$[1s^2]2s2p^68p$	4.4296	7.49
		$[1s^2]2s2p^69p$	4.4656	8.50
		$[1s^2]2s2p^610p$	4.4908	9.52

Clearly this process involves only one electron jump from  $2s$  to  $2p$  from the inner shell and therefore occurs with higher probability as compared to other resonances Mg III ( $2s2p^6\ ^2S^e$ ) $ns, n > 3$  and Mg III ( $2s2p^6\ ^2S^e$ ) $nd, n \geq 3$  which involves two electron jumps. Resonances of this type involving one electron jump are also noted by Yan and Seaton [2] and are referred as PEC resonances. We get two Rydberg series [Mg IV ( $2s^12p^6\ ^2S^e$ ) $ns$ ]  $^1S^e$  and [Mg IV ( $2s^12p^6\ ^2S^e$ ) $nd$ ]  $^1D^e$  in case of photoionization of the  $1s^22s^22p^5\ 3s\ ^3P^0$  state. The position and effective quantum numbers for these Rydberg series are given in table 4. Here again we find of the first member of the series [Mg IV ( $2s^12p^6\ ^2S^e$ ) $3s$ ]  $^1S^e$  is quite high as compared to other. This resonance is again PEC as it involves one electron jump, i.e.  $2s$  to  $2p$  (core excitation). For photoabsorption from  $1s^22s^22p^5\ 3p\ ^3S^e$  excited state there is only one final  $LS\pi$  state, i.e.  $^3P^0$  is allowed by selection rule which leads to a single Rydberg series of autoionized series [Mg IV ( $2s^12p^6\ ^2S^e$ ) $np$ ]  $^3P^0$  converging to  $^2S^e$  valence excited state. Their position and effective numbers are listed in table 5.

## Acknowledgement

We are thankful to CSIR and UGC for financial support.

## References

- [1] K One, *Phys. Rev.* **A37**, 1337 (1986)  
B Denne, *Phys. Scr.* **T26**, 42 (1989)
- [2] Y Yan and M J Seaton, *J. Phys.* **B20**, 6409 (1987)
- [3] J Nilsen, *J. Quant. Spectrosc. Radiat. Transfer* **47**, 171 (1992)
- [4] B Rahmani, S Y Liu, K Yasuoka, H A Belbachir and S Ishii, *Can. J. Phys.* **77**, 994 (1999)
- [5] J Davis, R Clark, J P Apruzse and P C Kepple, *IEEE Trans. Plasma Sci.* **16**, 482 (1988)
- [6] J W Thornhill, J Davis, J P Apruzse and R Clark, *Appl. Opt.* **31**, 4940 (1992)

- [7] J M Esteva and G Mehlman, *Astrophys. J.* **193**, 747 (1974)
- [8] M Mohan, Le M Dourneuf, A Hibbert and P G Burk, *Phys. Rev.* **A57**, 3489 (1998)
- [9] M Mohan and A Hibbert, *Phys. Scr.* **44**, 158 (1991)
- [10] H S Chakraborty *et al*, *Phys. Rev. Lett.* **83**, 2151 (1999)
- [11] N S Scott and P G Burk, *J. Phys.* **B13**, 4299 (1980)  
P G Burke and K T Taylor, *J. Phys.* **B8**, 2620 (1975)
- [12] K A Berrington, P G Burke, M Le Dourneuf, K T Taylor and V Ky Ian, *Comut. Phys. Commun.* **14**, 367 (1978)
- [13] A Hibbert, M Mohan and M Le Dourneuf, *At. Nucl. Data Tables* **53**, 23 (1993)
- [14] Clementi and C Roetti, *At. Data Nucl. Data Tables* **14**, 177 (1974)
- [15] W C Martin and Z Zalubus, *J. Phys. Chem. Ref. Data* **8**, 817 (1979)
- [16] E P Wigner and Eisenbud, *Phys. Rev.* **72**, 29 (1947)
- [17] P G Burke and W D Robb, *Adv. At. Mol. Phys.* **11**, 143 (1975)
- [18] K A Berrington, W B Eissner and P H Norrington, *CPC* **92**, 290 (1995)
- [19] A F Starace, *Phys. Rev.* **A3**, 1242 (1971)
- [20] A F Starace, *Phys. Rev.* **A8**, 1141 (1973)